Optimal Virtual Array Length Under Position Imperfections

Mannesson, Anders; Bernhardsson, Bo; Yaqoob, Muhammad Atif; Tufvesson, Fredrik

Published in:
[Host publication title missing]

2014

Optimal Virtual Array Length Under Position Imperfections

Anders Mannesson
and Bo Bernhardsson
Dept. of Automatic Control
Lund University, SWEDEN
Email: firstname.lastname@control.lth.se

Muhammad Atif Yaqoob
and Fredrik Tufvesson
Dept. of Electrical and Information Technology
Lund University, SWEDEN
Email: firstname.lastname@eit.lth.se

***Abstract*—This article contains a study of how spatial errors and receiver imperfections affect the angle of arrival estimation accuracy for virtual antenna arrays. A virtual antenna array consists of one receiver element whose location is tracked as the element is moved and in this work, linear arrays are studied. If the location of the receiver is tracked using an inertial measurement unit, an interesting trade-off emerges. The array should extend as far as possible but since the position estimates from the unaided inertial measurement unit become increasingly uncertain over time, the angle of arrival estimation will deteriorate. Several algorithms are available for estimating the angle of arrival in such a scenario but the one used for evaluation here is a sparse enforcing least squares method.**

I. Introduction

Estimation of the angle of arrival (AoA) is of interest for many positioning algorithms. One way of determining AoA is to use an antenna array [1]. By having several stationary antenna elements at known locations, the phase difference of the received signal between them can be used to estimate the AoA. However, instead of using stationary antenna elements, a single antenna element can just as well be used as long as the position of the element is known when the received signal is sampled and the channel remains stationary during the movement. This configuration is known as a virtual antenna array [1]. Such an array has different properties compared to a real antenna array with respect to (w.r.t.) estimation accuracy and imperfections in the receiver. Two fundamental problems exist: tracking of the moving antenna with sufficient accuracy, and frequency errors in the receiver. In this work the impact of both is studied.

By using an inertial measurement unit (IMU) consisting of accelerometers and gyroscopes, the position of the moving antenna can be determined with dead reckoning, see Fig. 1 [2]. The gyroscope measures the angular velocity while the accelerometer measures the acceleration of the device. Integrating the gyroscope readings yields the orientation which is then used for rotating the accelerometer readings. Gravity can then be removed and the position is obtained by double integration of the residual. This scheme will not give reliable position estimates for any longer period of time [2]. Due to noise and offsets in the sensor readings, the orientation will be incorrectly estimated and thus gravity can never completely be removed from the accelerometer readings. Also, the random noise from the sensors will be integrated leading to increasing variance of the position estimates. A virtual array should, similar to a real antenna array, cover a large area for reliable AoA estimation [3]. However, since the position estimates of the elements will be incorrect using dead reckoning, the AoA estimates will be affected. When the position error becomes too large, it becomes necessary to use other algorithms estimating joint position and AoA, see *e.g.* [4] and [5], but the unaided virtual array can potentially be used for initialization of such algorithms. Also, if the receiver suffers from frequency errors leading to growing phase errors, this will affect the AoA estimation accuracy. It is therefore of interest to study if an optimal length of the IMU based virtual array can be found when these imperfections are taken into account.

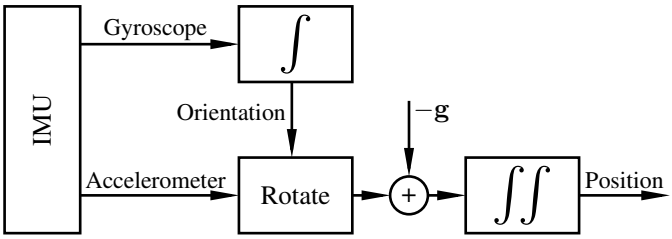

Fig. 1. Dead reckoning approach using an IMU. The gyroscope signal is integrated once to obtain orientation which is used for rotating the accelerometer signal from body coordinates to world coordinates. Gravity $\mathbf{g}$ is removed after rotation and the residual is integrated twice to obtain position.

II. Modeling

A. Signal Model

Let's assume R narrowband sources, transmitting at the same frequency, and a receiver element located in the far field region. After downconversion and sampling, the received baseband signal can be written as

$$y[n] = \sum_{r=1}^{R} \alpha_r e^{-i\gamma\langle u(\phi_r), p[n]\rangle} + e[n], \quad n = 1, \ldots, N, \quad (1)$$

where α_r is the complex channel gain associated with source r, $u(\phi_r)$ is a unit vector pointing in the azimuth direction of ϕ_r, $p[n]$ is the 2D position of the receiver element at time n, $e[n]$ is the noise, and $\gamma = 2\pi\lambda^{-1}$, where λ is the wavelength

of the carrier frequency. By collecting the measurements into a vector, the relationship can be written as

$$Y = \Phi X + E, \tag{2}$$

where $Y = [y[1], \ldots, y[N]]^T$, $X = [\alpha_1, \ldots, \alpha_R]^T$, and

$$\Phi = \begin{bmatrix} e^{-i\gamma\langle u(\phi_1), p[1]\rangle} & \ldots & e^{-i\gamma\langle u(\phi_R), p[1]\rangle} \\ \vdots & \ddots & \vdots \\ e^{-i\gamma\langle u(\phi_1), p[N]\rangle} & \ldots & e^{-i\gamma\langle u(\phi_R), p[N]\rangle} \end{bmatrix} \in \mathbb{C}^{N\times R}. \tag{3}$$

The column vectors in Φ are referred to as steering vectors.

Assume that there is a frequency offset between the local oscillator of the receiver and the transmitted carrier frequency. The difference between the two frequencies will be integrated into a phase drift. If all impinging rays are subject to the same drift, the frequency error can be added to the signal (1) as

$$y[n] = \sum_{r=1}^{R} \alpha_r e^{-i(\gamma\langle u(\phi_r), p[n]\rangle + n\delta)} + e[n], \quad n = 1, \ldots, N, \tag{4}$$

where δ is the frequency error measured in radians per sample.

As can be seen in (4), the frequency error affects the phase of the received signal in the same way as a movement does. Assuming one impinging ray, the frequency error can be interpreted as an offset in the AoA according to

$$\langle u(\phi), v\rangle + \delta = \langle u(\tilde{\phi}), v\rangle, \tag{5}$$

where $\tilde{\phi} - \phi$ is the offset and v is the velocity of the receiver.

In a real scenario, the frequency error would be estimated and removed. If the estimated value does not cancel the frequency error fully, a residual will be left, corresponding to the frequency error added here. For simplicity, the frequency error is assumed to be constant throughout the measurement period in this article.

B. Inertial Navigation System

IMUs are classified based on the noise levels of the sensors. The cheapest ones are usually referred to as *consumer* grade while more expensive ones are called *industrial* or *tactical* grade [2]. IMUs of consumer grade can be built using MEMS technology and are therefore suitable for integration in consumer electronics. Typical values for the standard deviation of the Gaussian noise processes on the accelerometer and gyroscope are 0.2 m/s/$\sqrt{\text{h}}$ and 2 °/$\sqrt{\text{h}}$ respectively. More noise sources can be modeled, *e.g.*, random walk noise processes [6], but these noise sources will not affect the position estimates for the simulation times considered in this paper. Therefore, these additional noise sources are left unmodeled.

If the dead reckoning scheme in Fig. 1 is implemented and an IMU of consumer grade at rest is simulated, the integrated noise leads to position errors as shown in Fig. 2. For the simulation, a carrier wavelength of 16.7 cm is used. In the figure, the mean deviation of the true position is shown vs. time. The error bars indicates one standard deviation confidence interval, using the typical noise values given earlier. It is clear that the errors are small in the beginning and then grow rapidly, mostly due to errors in the orientation which results in residuals after gravity has been subtracted.

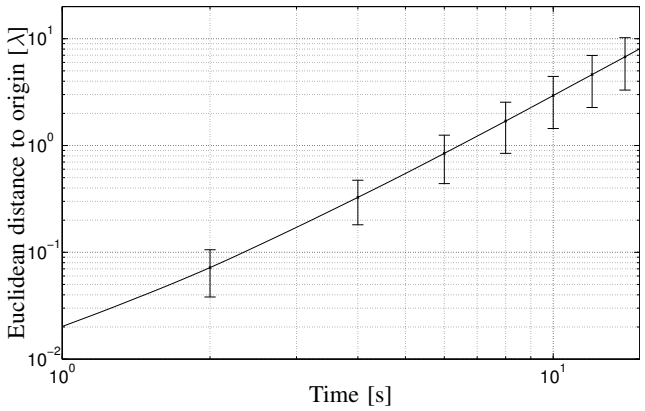

Fig. 2. Simulated position error and standard deviation using dead reckoning for a typical IMU of consumer grade. Note that the distance is presented in the unit λ and after 5 seconds the estimated position error is approximately 0.6 λ with a standard deviation of 0.25 λ with λ = 16.7 cm.

III. Estimating Angle of Arrival

Estimating the AoA using an antenna array is a well researched area with many contributions. Classic algorithms such as Capon's beamformer [7], MUSIC [8], and SAGE [9] are all well established. A simple, yet efficient way to estimate the AoA is to divide the unit circle into grid points and then solve the problem with a least squares approach together with a regularization term to enforce a sparse solution [10]. If the unit circle is gridded into M grid points, the problem can be formulated as

$$\underset{X\in\mathbb{C}^{M\times 1}}{\text{minimize}} \quad \|Y - \Phi_M X\|_2^2, + \kappa\|WX\|_1 \tag{6}$$

where $\Phi_M \in \mathbb{C}^{N\times M}$ contains the steering vectors for all M grid points at the different positions of the elements, κ is a design parameter, and $W \in \mathbb{R}^{M\times M}$ is a weighing matrix with $w = [w_1, w_2, \ldots, w_M]^T$ on its main diagonal. The weights are initialized as ones and (6) is solved. The weights are then recalculated according to

$$w'_m = \frac{1}{|x_m| + \epsilon}, \quad m = 1, \ldots, M, \tag{7}$$

where w'_m are the weights used the second time (6) is solved, and ϵ controls the maximum weight that can be set [10]. This procedure can be repeated several times but here the problem is solved twice. The regularization has the effect that small elements in X will be weighted heavier than larger elements, forcing the algorithm to find an even more sparse solution to X compared to traditional ℓ_1 regularization [10]. The problem (6) is convex in X so convex optimization can efficiently be used to solve it [11]. Note that the increasing uncertainty in position embedded in the steering vectors is not taken into account when (6) is solved.

IV. Simulation

A. Configuration

To evaluate the trade-off described before, the dead reckoning scheme from Fig. 1 is implemented and the so called iterative re-weighted optimization problem (6) is solved. The noise levels for the accelerometer and gyroscope signals are chosen to match an IMU of consumer grade.

The radio environment is configured with two rays directed towards the array at angle $\phi_1 = 45°$ and $\phi_2 = 125°$ with amplitudes of $|\alpha_1| = 2$ and $|\alpha_2| = 1$ respectively. The wavelength λ is set to 16.7 cm, corresponding to 1795 MHZ, for all simulations. The signal to noise ratio (SNR) of the radio signal is altered to investigate its effect on the AoA estimation. The search set for possible AoA is chosen as $[0, \pi]$ divided into 200 equidistant grid points.

The virtual array is formed by moving the receiver antenna at a constant velocity along a straight line. For every second, 12 new samples of the radio signal are added onto the data vector Y and used for evaluating the AoA. The two largest peaks in the solution to (6) are identified and denoted by $\hat{\phi}_1$ and $\hat{\phi}_2$ respectively. The two angles are used to calculate the steering vectors in the matrix $\hat{\Phi}$ and then the least squares solution of $Y = \hat{\Phi}X$ is calculated to retrieve the complex amplitudes $|\hat{\alpha}_1|$ and $|\hat{\alpha}_2|$. The AoA estimation problem in (6) is solved for 1000 different statistical realizations and the root mean square error (RMSE) for the theta estimation is calculated as

$$\text{RMSE} = \left(\frac{1}{2M} \sum_{r=1}^{2} \sum_{m=1}^{M} |\hat{\phi}_r^m - \phi_r|^2 \right)^{1/2} \tag{8}$$

where ϕ_r is the true AoA and $\hat{\phi}_r^m$ is the solution of the m:th Monte Carlo simulation. RMSE for the amplitude estimation is calculated similarly.

V. Results

The results from the simulations with the described model and configuration are presented in Fig. 3 to Fig. 6. In Fig. 3, RMSE for $\hat{\phi}$ and $|\hat{\alpha}|$ is shown for three different levels of constant frequency error when the device is moved with a velocity of 5 λ/s. The result is good up to array sizes of 25 λ, corresponding to 5 seconds of movement. From Fig. 2, the error at that time is 0.6 λ. For longer arrays, the performance deteriorates rapidly. Also, the phase drift is clearly setting a limit, as discussed in Section II-A. From (5), the contribution to RMSE in AoA for the different levels of frequency error becomes 15°, 7.5°, and 1.5° for 72 $°/\lambda$, 36 $°/\lambda$, and 7.2 $°/\lambda$ respectively which closely matches the result in Fig. 3. Looking at RMSE for the amplitude, there is not much difference between the three simulations. The conclusion is that the frequency error does not affect the amplitude estimation the same way as it does for AoA estimation.

If the velocity of the device is increased to 10 λ/s, the performance for both AoA and amplitude does not deteriorate for sizes up to 50 λ. The reason is that the position errors do not reach the same uncertainty as before since the movement is completed in 5 seconds compared to 10 seconds before.

To study influence of SNR, two levels of frequency error

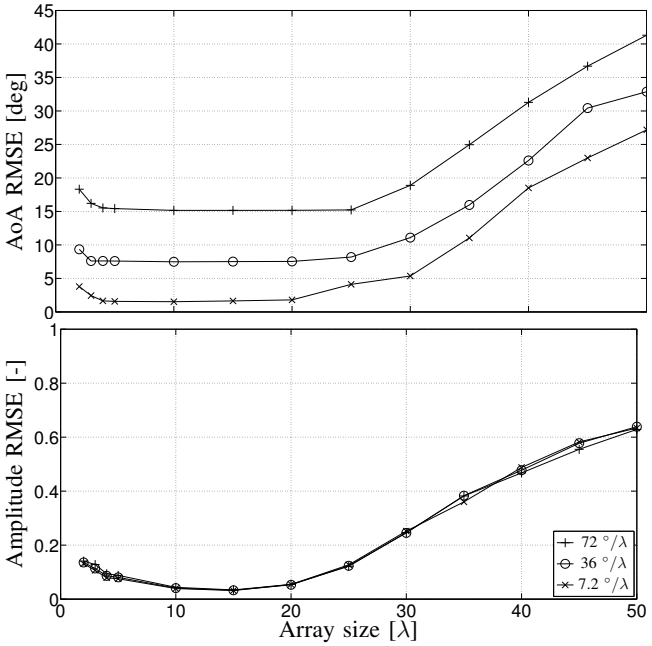

Fig. 3. The upper panel shows RMSE for AoA estimation w.r.t. array size while the lower shows RMSE of amplitude estimation. The velocity of the device is set to 5 λ/s and the SNR is 20 dB. The lines indicate the level of frequency error in the simulation. Note that RMSE of AoA and amplitude deteriorate at array lengths larger than 25 λ for all levels of frequency error. Also, a smaller frequency error allows a longer array size considering AoA RMSE, *i.e.*, a similar RMSE is observed for an array length of 40 λ with a frequency error of 7.2 $°/\lambda$ as at a length of 30 λ with 72 $°/\lambda$ error.

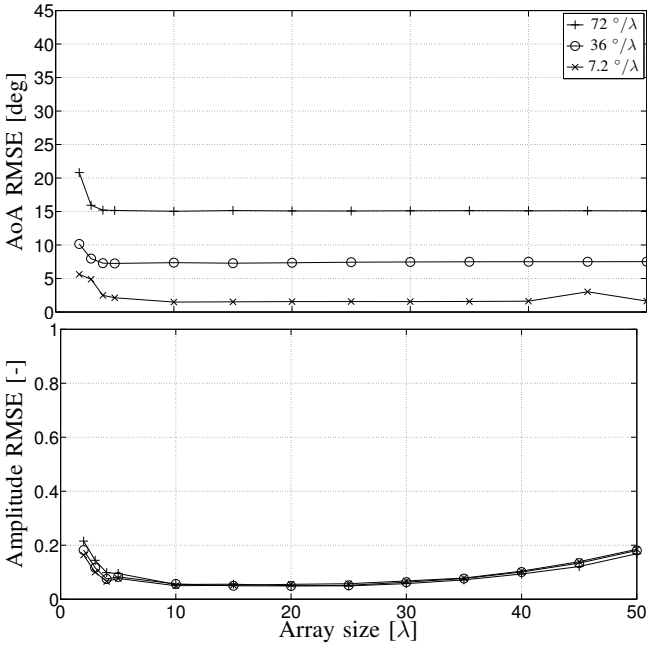

Fig. 4. Same as Fig. 3 but with velocity of 10 λ/s. The AoA shows no signs of deterioration with increasing length of the array. There is a small impact on the amplitude.

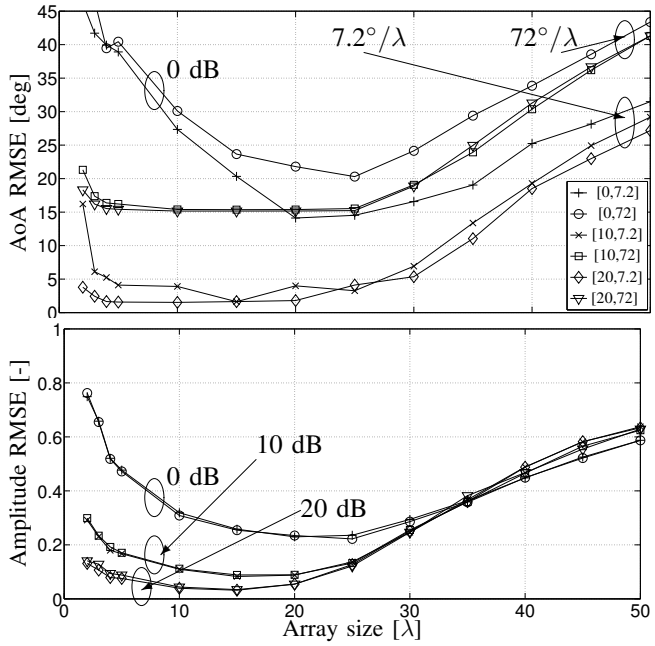

Fig. 5. The upper panel shows RMSE for AoA estimation w.r.t. array size while the lower shows amplitude estimation. The lines indicate the level of SNR and phase drift in the simulation as [dB,$^\circ/\lambda$]. Note that RMSE of AoA deteriorates at array lengths larger than 25 λ, independently of SNR.

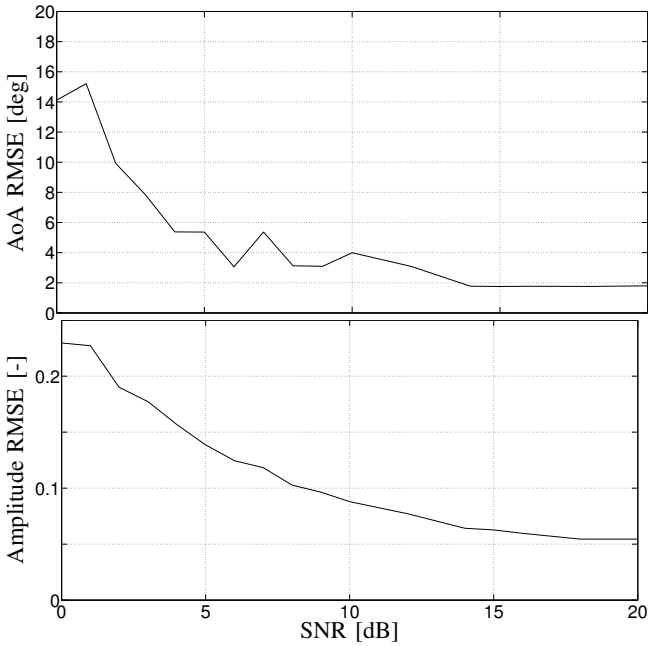

Fig. 6. The upper panel shows RMSE for AoA, the lower shows RMSE for amplitude, both vs. SNR. The velocity of the receiver is chosen to 5 λ/s, the array length is 20 λ, and frequency error is 7.2$^\circ/\lambda$. For AoA the performance deteriorates rapidly for SNR below 5dB. For amplitude, the performance is decreasing slowly with worsening SNR.

are chosen, 7.2$^\circ/\lambda$ and 72$^\circ/\lambda$, and scenarios with SNR of 0 dB, 10 dB, and 20 dB are simulated with velocity 5 λ/s.

From Fig. 5 it is clear that there is some impact from the SNR of the radio signal. For SNR values of 10 dB and 20 dB, the performance for AoA is similar. Once again, the frequency error sets a lower limit of how well the AoA can be estimated. However, at 0 dB the performance is much worse compared to the scenarios with better SNR. There is a breakpoint where the noise affects the estimation more than the frequency error. For the amplitude estimation, there is a clear dependence between accuracy and SNR for short arrays. For longer arrays, larger than 25 λ, the difference becomes smaller and for long arrays there is no difference.

To investigate the dependence of SNR for AoA estimation, a frequency error of 7.2 $\lambda/^\circ$ is chosen and an array of fixed length of 20 λ is used. The SNR is varied from 20 dB to 0 dB and presented in Fig. 6. RMSE for amplitude increases smoothly as the SNR gets worse. For the AoA, there is a rapid change at 5 dB where the performance becomes much worse.

VI. Conclusion

The article shows how a virtual antenna array, consisting of a single receiver element and an unaided IMU can be used to estimate angle of arrival. Imperfections in the IMU, such as noise in the sensors are considered as well as noise and frequency error in the radio receiver. As expected, there is a clear trade-off between array length and estimation accuracy which is dependent on noise levels, speed of the receiver, and frequency error. The general conclusion is that the combination of an unaided IMU and a single receiver element has the potential to deliver an initial estimate which can be used in more advanced algorithms estimating joint pose and AoA, [5].

Acknowledgment

The authors are part of The Lund Linköping Initiative on IT (ELLIIT) Excellence Center, supported by the Swedish Government. Support from the LCCC Linnaeus Center, Swedish Research Council, and Vetenskapsrådet project 2012-42391-93793-23, is also acknowledged.

References

[1] A. F. Molisch, *Wireless Communications*. Wiley, 2005.
[2] P. D. Groves, *Principles of GNSS, inertial, and multisensor integrated navigation systems*. Artech House, 2013.
[3] A. Dogandžić and A. Nehorai, "Cramér-Rao bounds for estimating range, velocity, and direction with an active array," *IEEE Trans. Signal Process.*, vol. 49, no. 6, pp. 1122–1137, Jun. 2001.
[4] A. Mannesson, M. A. Yaqoob, B. Bernhardsson, and F. Tufvesson, "Radio and IMU based indoor positioning and tracking," in *IEEE Int. Conf. Systems, Signals and Image Processing*, Apr. 2012, pp. 32–35.
[5] A. Mannesson, "Joint pose and radio channel estimation," Dept. of Automatic Control, Lund Uni., Sweden," Licentiate Thesis, Jun. 2013.
[6] O. Woodman, "Pedestrian localisation for indoor environments," Ph.D. dissertation, Uni. of Cambridge, Computer Laboratory, Sep. 2010.
[7] J. Capon, "High-resolution frequency-wavenumber spectrum analysis," *Proc. IEEE*, vol. 57, no. 8, pp. 1408–1418, 1969.
[8] R. Schmidt, "Multiple emitter location and signal parameter estimation," *IEEE Trans. Antennas Propag.*, vol. 34, no. 3, pp. 276–280, Mar. 1986.
[9] J. A. Fessler and A. O. Hero, "Space-alternating generalized expectation-maximization algorithm," *IEEE Trans. Signal Process.*, vol. 42, no. 10, pp. 2664–2677, Oct. 1994.
[10] E. J. Candes, M. B. Wakin, and S. P. Boyd, "Enhancing sparsity by reweighted ℓ_1 minimization," *Journal of Fourier Analysis and Applications*, vol. 14, no. 5, pp. 877–905, 2008.
[11] S. Boyd and L. Vandenberghe, *Convex optimization*. Cambridge university press, 2004.